

Distributed Transfer Function Method for Analysis of Cylindrical Shells

Jianping Zhou* and Bingen Yang†

University of Southern California, Los Angeles, California 90089-1453

A distributed transfer function method for static and dynamic analysis of general cylindrical shells is proposed. The distributed transfer functions of a cylindrical shell, the Laplace transforms of the shell Green's functions, are first derived. Stepped shells composed of a finite number of serially connected shell segments are then synthesized using these transfer functions. In this formulation, exact and closed-form solutions for various static and dynamic problems of cylindrical shells under arbitrary boundary conditions and external loads are obtained. Numerical examples are provided to show the efficiency and flexibility of the transfer function method.

I. Introduction

CYLINDRICAL shells are the basic elements of many structures and machines in aerospace, civil, mechanical, and marine engineering. The static and dynamic problems of cylindrical shells have been extensively studied in the past decade. Irie et al.¹ studied free vibration of a point-supported cylindrical shell by the Ritz method. Yamada et al.² applied the transfer matrix method to vibration and stability problems of orthotropic circular cylindrical shells subjected to axial loads. Sheinman and Weissman³ and Koga⁴ examined the effects of different boundary conditions on the shell dynamic characteristics. Koga and Morimatsu⁵ and Lou and Yaniv⁶ investigated the buckling of cylindrical shells under external pressure, axial compression, and bending loads. Thangaratnam et al.⁷ performed a finite element analysis of shell thermal buckling. Huang and Hsu⁸ proposed a receptance method for vibration analysis of rotating cylindrical shells. Narita et al.⁹ and Heyliger and Jilani¹⁰ studied vibrations of angle-ply cylindrical shells having arbitrary edges. Birman¹¹ addressed the nonlinear bending problem of laminated cylindrical shells subjected to axisymmetric radial pressure and axial and torsional loadings. Miyazaki and Hagihara¹² conducted both analytical and experimental investigations of creep buckling phenomena of cylindrical shells. All of these studies have greatly increased our understanding of the behavior of cylindrical shells.

The purpose of this study is to develop a unified analytical and numerical method for modeling and analysis of general cylindrical shells. In the previous research on cylindrical shells, approximate and asymptotic methods have been widely used; comparably, exact and closed-form solution methods have not been well developed, with notable exceptions in Chaudhuri and Abu-Arja¹³ and Christoforou and Swanson.¹⁴ Although advanced computer technology and powerful numerical algorithms, such as finite element methods (FEM), make it possible to analyze complicated flexible systems, analytical methods are always desirable, for they yield more accurate results and deeper physical understanding of structures.

This paper presents a distributed transfer function formulation. The distributed transfer functions of a flexible system are the Laplace transforms of the system Green's functions.¹⁵ As a new modeling and analysis tool for flexible mechanical systems, the distributed transfer function method has attracted great attention recently.¹⁶ As shall be shown in this paper, the proposed transfer function method has the following special features:

1) The transfer function method provides exact and closed-form solutions for static deflection, free vibration, buckling, and frequency response of cylindrical shells under arbitrary boundary conditions and external loads.

2) The transfer function method represents various linear models of cylindrical shells (Love type, Donnell–Mushtari type, etc.) and characterizes different physical properties, such as gyroscopic effects from a spinning shell, isotropic/anisotropic and elastic/viscoelastic material, and nonuniformly distributed damping.

3) The distributed transfer functions can be used to synthesize stepped cylindrical shells, shells with continuously varying thickness, and shells with stiffeners.

4) The transfer function method is convenient in numerical simulation and computer coding. Different systems, boundary conditions, and external loads are systematically treated in one simple and compact matrix form, as in finite element analysis.

The remaining sections are arranged as follows. In Sec. II, the exact distributed transfer functions of a circular cylindrical shell are derived, and their application in static and dynamic analysis is discussed. In Sec. III, the transfer functions obtained are used to analyze stepped shells composed of several serially connected shell segments. Two synthesis procedures are proposed: the connection matrix method and the nodal displacement method. The transfer function formulation is applied to shells of the Donnell–Mushtari type in Sec. IV, and the numerical examples are presented in Sec. V.

II. Distributed Transfer Function Formulation

To demonstrate the transfer function method, we start with a homogeneous circular cylindrical shell of length L and radius R , as shown in Fig. 1. The governing equations for the small deformation of the shell have the form

$$\sum_{k=1}^3 \sum_{i=0}^{n_k} \sum_{j=0}^i L_{mkij} \frac{\partial^i}{\partial x^{i-j} \partial \theta^j} u^k(x, \theta, t) = f^m(x, \theta, t) \quad m = 1, 2, 3 \quad (1)$$

where u^1 , u^2 , and u^3 are the shell displacements in the longitudinal (x —), circumferential (θ —), and radial (z —) directions, respectively; $f^m(x, \theta, t)$ are the external loads applied to the shell; L_{mkij} are the temporal differential operators defined by

$$L_{mkij} = A_{mkij} \frac{\partial^2}{\partial t^2} + B_{mkij} \frac{\partial}{\partial t} + C_{mkij} \quad (2)$$

n_k is the highest order of spatial differentiation of u^k ; and A_{mkij} , B_{mkij} , and C_{mkij} are the constants describing the geometric and material properties of the shell. Equation (1) in general represents various linear theories of cylindrical shells.

Received May 2, 1994; accepted for publication Oct. 6, 1994. Copyright © 1994 by the American Institute of Aeronautics and Astronautics, Inc. All rights reserved.

*Visiting Professor, Department of Mechanical Engineering; currently Professor, Department of Astronautics, National University of Defense Technology, Changsha, Hunan 410073, People's Republic of China.

†Assistant Professor, Department of Mechanical Engineering. Member AIAA.

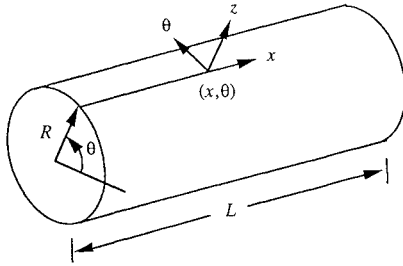


Fig. 1 A homogeneous cylindrical shell.

The boundary conditions specified at the two ends of the shell have the form

$$\left[\sum_{k=1}^3 \sum_{i=0}^{n_k-1} \sum_{j=0}^i \beta_{lkij} \frac{\partial^i u^k(x_\alpha, \theta, t)}{\partial x^{i-j} \partial \theta^j} \right]_{x=x_\alpha} = \lambda^l(\theta, t) \quad l = 1, 2, \dots, n_b \quad (3)$$

where $x_\alpha = 0$ and L for $\alpha = 1$ and 2 , respectively; β_{lkij} are constants, and $\lambda^l(\theta, t)$ are the given functions representing the boundary disturbances. The number of boundary conditions $n_b = n_1 + n_2 + n_3$ and in most situations is eight. The initial conditions are

$$u^k(x, \theta, t) = u_0^k(x, \theta), \quad \frac{\partial}{\partial t} u^k(x, \theta, t) = u_1^k(x, \theta) \quad k = 1, 2, 3 \quad (4)$$

In the proposed transfer function formulation, the shell displacements are first expanded in Fourier series in the circumferential direction θ , and then Laplace transformed with respect to time t . The Fourier series of the shell displacements, external loads, and initial and boundary disturbances are given by

$$u^k(x, \theta, t) = \sum_{n=0}^{\infty} [u_{1,n}^k(x, t) \cos n\theta + u_{2,n}^k(x, t) \sin n\theta] \quad k = 1, 2, 3 \quad (5a)$$

$$f^m(x, \theta, t) = \sum_{n=0}^{\infty} [f_{1,n}^m(x, t) \cos n\theta + f_{2,n}^m(x, t) \sin n\theta] \quad m = 1, 2, 3 \quad (5b)$$

$$u_0^k(x, \theta) = \sum_{n=0}^{\infty} [u_{1,n}^{k,0}(x) \cos n\theta + u_{2,n}^{k,0}(x) \sin n\theta] \quad k = 1, 2, 3 \quad (5c)$$

$$u_1^k(x, \theta) = \sum_{n=0}^{\infty} [u_{1,n}^{k,1}(x) \cos n\theta + u_{2,n}^{k,1}(x) \sin n\theta] \quad k = 1, 2, 3 \quad (5d)$$

$$\lambda^l(\theta, t) = \sum_{n=0}^{\infty} [\lambda_{1,n}^l(t) \cos n\theta + \lambda_{2,n}^l(t) \sin n\theta] \quad l = 1, 2, \dots, n_b \quad (5e)$$

where $u_{1,n}^k(x, t)$ and $u_{2,n}^k(x, t)$ are the unknown displacement functions to be determined; all of the other functions are known from the specified loads and initial and boundary conditions. Substituting the Fourier series into Eq. (1) and equating the coefficients of the sine and cosine terms on both sides yield an infinite number of decoupled equations

$$\sum_{k=1}^3 \sum_{i=0}^{n_k} \left[\sum_{j=0}^{\lfloor \frac{i}{2} \rfloor} L_{mki(2j)} (-1)^j n^{2j} \frac{\partial^{i-2j} u_{1,n}^k}{\partial x^{i-2j}} + \sum_{j=1}^{\lfloor \frac{i+1}{2} \rfloor} L_{mki(2j-1)} (-1)^{j+1} n^{2j-1} \frac{\partial^{i-(2j-1)} u_{2,n}^k}{\partial x^{i-(2j-1)}} \right] = f_{1,n}^m(x, t) \quad (6a)$$

$$\sum_{k=1}^3 \sum_{i=0}^{n_k} \left[\sum_{j=0}^{\lfloor \frac{i}{2} \rfloor} L_{mki(2j)} (-1)^j n^{2j} \frac{\partial^{i-2j} u_{2,n}^k}{\partial x^{i-2j}} + \sum_{j=1}^{\lfloor \frac{i+1}{2} \rfloor} L_{mki(2j-1)} (-1)^j n^{2j-1} \frac{\partial^{i-(2j-1)} u_{1,n}^k}{\partial x^{i-(2j-1)}} \right] = f_{2,n}^m(x, t) \quad (6b)$$

where $m = 1, 2, 3, n = 1, 2, \dots$, and $[x]$ denotes the integer part of x . Note that $u_{i,n}^k(x, t)$ and $u_{j,m}^k(x, t)$ do not couple if $n \neq m$. Laplace transform of Eq. (6) with respect to time t leads to

$$\sum_{k=1}^3 \sum_{i=0}^{n_k} \left[\sum_{j=0}^{\lfloor \frac{i}{2} \rfloor} D_{mki(2j)}(s) (-1)^j \frac{\partial^{i-2j} \tilde{u}_{1,n}^k}{\partial x^{i-2j}} + \sum_{j=1}^{\lfloor \frac{i+1}{2} \rfloor} D_{mki(2j-1)}(s) (-1)^{j+1} \frac{\partial^{i-(2j-1)} \tilde{u}_{2,n}^k}{\partial x^{i-(2j-1)}} \right] = \tilde{f}_{1,n}^m(x, s) + \tilde{g}_{1,n}^m(x, s) \quad (7a)$$

$$\sum_{k=1}^3 \sum_{i=0}^{n_k} \left[\sum_{j=0}^{\lfloor \frac{i}{2} \rfloor} D_{mki(2j)}(s) (-1)^j \frac{\partial^{i-2j} \tilde{u}_{2,n}^k}{\partial x^{i-2j}} + \sum_{j=1}^{\lfloor \frac{i+1}{2} \rfloor} D_{mki(2j-1)}(s) (-1)^j \frac{\partial^{i-(2j-1)} \tilde{u}_{1,n}^k}{\partial x^{i-(2j-1)}} \right] = \tilde{f}_{2,n}^m(x, s) + \tilde{g}_{2,n}^m(x, s) \quad (7b)$$

where the tilde stands for Laplace transformation, the complex numbers

$$D_{mki j}(s) = (A_{mki j} s^2 + B_{mki j} s + C_{mki j}) n^j$$

and $\tilde{g}_{2,n}^m(x, s)$ and $\tilde{g}_{1,n}^m(x, s)$ are the functions of $u_{\alpha,n}^{k,0}(x)$ and $u_{\alpha,n}^{k,0}(x)$ in Eqs. (5c) and (5d), representing the shell initial disturbances.

Apply the same procedure to Eq. (3) to obtain the boundary conditions for the displacement functions $\tilde{u}_{1,n}^k(x, s)$ and $\tilde{u}_{2,n}^k(x, s)$ at the two ends of the shell:

$$\sum_{k=1}^3 \sum_{i=0}^{n_k-1} \left[\sum_{j=0}^{\lfloor \frac{i}{2} \rfloor} (-1)^j n^{2j} \beta_{lki(2j)} \frac{\partial^{i-2j} \tilde{u}_{1,n}^k}{\partial x^{i-2j}} + \sum_{j=1}^{\lfloor \frac{i+1}{2} \rfloor} (-1)^{j+1} n^{2j} \beta_{lki(2j-1)} \frac{\partial^{i-(2j-1)} \tilde{u}_{2,n}^k}{\partial x^{i-(2j-1)}} \right]_{x=x_\alpha} = \tilde{\lambda}_{1,n}^l(s) \quad (8a)$$

$$\sum_{k=1}^3 \sum_{i=0}^{n_k-1} \left[\sum_{j=0}^{\lfloor \frac{i}{2} \rfloor} (-1)^j n^{2j} \beta_{lki(2j)} \frac{\partial^{i-2j} \tilde{u}_{2,n}^k}{\partial x^{i-2j}} + \sum_{j=1}^{\lfloor \frac{i+1}{2} \rfloor} (-1)^j n^{2j} \beta_{lki(2j-1)} \frac{\partial^{i-(2j-1)} \tilde{u}_{1,n}^k}{\partial x^{i-(2j-1)}} \right]_{x=x_\alpha} = \tilde{\lambda}_{2,n}^l(s) \quad (8b)$$

where $l = 1, 2, \dots, n_b; \alpha = 1, 2$; and $n = 1, 2, \dots$; and $\tilde{\lambda}_{\alpha,n}^l(s)$ is the Laplace transform of $\lambda_{\alpha,n}^l(t)$.

Introduce the state-space vector

$$\eta_n = \{ \eta_{1,1,n}^T \quad \eta_{1,2,n}^T \quad \eta_{2,1,n}^T \quad \eta_{2,2,n}^T \quad \eta_{3,1,n}^T \quad \eta_{3,2,n}^T \}^T \in \mathbb{C}^{2N} \quad (n = 1, 2, \dots) \quad (9a)$$

where $N = n_b = n_1 + n_2 + n_3$, n is the shell circumferential wave number, and

$$\eta_{k,i,n} = \left[u_{i,n}^k \quad \frac{\partial}{\partial x} u_{i,n}^k \quad \cdots \quad \frac{\partial^{n_k-1}}{\partial x^{n_k-1}} u_{i,n}^k \right]^T \in C^{n_k} \quad (i = 1, 2; \quad k = 1, 2, 3) \quad (9b)$$

With Eqs. (9), Eqs. (7) and (8) are cast into a state-space form

$$\frac{\partial}{\partial x} \eta_n(x, s) = F_n(s) \eta_n(x, s) + \tilde{f}_n(x, s) + \tilde{g}_n(x, s) \quad x \in (0, L) \quad (10a)$$

$$M_n(s) \eta_n(0, s) + N_n(s) \eta_n(L, s) = \gamma_n(s) \quad (10b)$$

with $F_n(s)$, $M_n(s)$, $N_n(s) \in C^{2N \times 2N}$ composed of the coefficients in Eqs. (7) and (8), and $\tilde{f}_n(x, s)$, $\tilde{g}_n(x, s)$, $\gamma_n(s) \in C^{2N}$ consisting of the external and boundary excitation functions; see the Appendix.

Equations (10) form a boundary-value problem. According to Yang and Tan,¹⁷ the exact and closed-form solution to Eqs. (10) is

$$\eta_n(x, s) = \int_0^L G_n(x, \xi, s) [\tilde{f}_n(\xi, s) + \tilde{g}_n(\xi, s)] d\xi + H_n(x, s) \gamma_n(s) \quad (11)$$

where the distributed transfer functions

$$G_n(x, \xi, s) = \begin{cases} H_n(x, s) M_n(s) e^{-F_n(s)\xi}, & \xi \leq x \\ -H_n(x, s) N_n(s) e^{F_n(s)(L-\xi)}, & \xi > x \end{cases} \quad (12a)$$

$$H_n(x, s) = e^{F_n(s)x} [M_n(s) + N_n(s) e^{F_n(s)L}]^{-1} \quad (12b)$$

Once the solution $\eta_n(x, s)$ is obtained, the displacement functions can be expressed as

$$\begin{aligned} \tilde{u}_{1,n}^1(x, s) &= \eta_n^1(x, s), & \tilde{u}_{2,n}^1(x, s) &= \eta_n^{n_1+1}(x, s) \\ \tilde{u}_{1,n}^2(x, s) &= \eta_n^{2n_1+1}(x, s), & \tilde{u}_{2,n}^2(x, s) &= \eta_n^{2n_1+n_2+1}(x, s) \\ \tilde{u}_{1,n}^3(x, s) &= \eta_n^{2n_1+2n_2+1}(x, s), & \tilde{u}_{2,n}^3(x, s) &= \eta_n^{2n_1+2n_2+n_3+1}(x, s) \end{aligned}$$

where $\eta_n^j(x, s)$ is the j th element of $\eta_n(x, s)$. Thus, by Eq. (5a), the s -domain displacements of the cylindrical shell are

$$u^1(x, s) = \sum_{n=0}^{\infty} [\eta_n^1(x, s) \cos n\theta + \eta_n^{n_1+1}(x, s) \sin n\theta] \quad (13a)$$

$$u^2(x, s) = \sum_{n=0}^{\infty} [\eta_n^{2n_1+1}(x, s) \cos n\theta + \eta_n^{2n_1+n_2+1}(x, s) \sin n\theta] \quad (13b)$$

$$u^3(x, s) = \sum_{n=0}^{\infty} [\eta_n^{2n_1+2n_2+1}(x, s) \cos n\theta + \eta_n^{2n_1+2n_2+n_3+1}(x, s) \sin n\theta] \quad (13c)$$

In the above derivation, no approximation has been made; the transfer function formulation provides an exact and closed-form solution method. This method is fairly general, for different shell models and arbitrary boundary conditions are systematically treated through easy formation of the matrices $F_n(s)$, $M_n(s)$, and $N_n(s)$. As a result, the method is convenient in numerical simulation and computer coding.

The transfer function formulation can be applied to the free vibration and buckling problems of cylindrical shells. For free vibration, the characteristic equations of the shell, by Eq. (12b), are

$$\det[M_n(s) + N_n(s) e^{F_n(s)L}] = 0, \quad n = 1, 2, \dots \quad (14)$$

whose roots are the eigenvalues of the shell. The corresponding eigenfunctions are given by

$$\eta_n(x, \omega) = e^{F_n(\omega)x} \psi, \quad x \in (0, L) \quad (15a)$$

where ω is a root of Eq. (14), and the complex vector $\psi \in C^{2N}$ satisfies

$$[M_n(\omega) + N_n(\omega) e^{F_n(\omega)L}] \psi = 0 \quad (15b)$$

Note that the vector function $\eta_n(x, \omega)$ in Eq. (15a) simultaneously presents the modal distributions of the shell displacements and internal forces.

In the buckling problem, the matrices M_n , N_n , and F_n are functions of a load parameter p , namely, $M_n = M_n(s; p)$, $N_n = N_n(s; p)$, and $F_n = F_n(s; p)$. The shell buckling is analyzed by letting $s = 0$ in Eq. (14):

$$\det[M_n(0; p) + N_n(0; p) e^{F_n(0; p)L}] = 0 \quad (16)$$

The solutions p_k from Eq. (16) are the buckling loads; the corresponding buckling mode shapes can be obtained following Eqs. (15). In addition, for a prestressed shell subjected to a given load \bar{p} , its natural frequencies in vibration can be determined from the following characteristic equation:

$$\det[M_n(s; \bar{p}) + N_n(s; \bar{p}) e^{F_n(s; \bar{p})L}] = 0 \quad (17)$$

The frequency response of the shell subjected to harmonic excitations can be expressed by the transfer functions. For instant, under an excitation of frequency ω , the shell longitudinal vibration is $u^1(x, t) = \sum_{n=0}^{\infty} \{\eta_n^1(x, j\omega) \cos n\theta + \eta_n^{n_1+1}(x, j\omega) \sin n\theta\} e^{j\omega t}$, where $j = \sqrt{-1}$. Moreover, the transfer functions can be directly used to predict the stability of the cylindrical shell under various forcing sources and to design active controllers and smart structure mechanisms.

III. Synthesis of Stepped Cylindrical Shells

A stepped cylindrical shell in Fig. 2 is composed of n_s serially connected shell segments of radius R , length l_i , and thickness h_i , respectively. Here, the geometry and material parameters are the same within each shell segment but may change from segment to segment. Stepped shells have various engineering applications and can be used to achieve minimum weight design of structures and machines. Moreover, stepped shells can model cylindrical shells with stiffeners¹⁸ and shells of continuously varying thickness along its longitudinal direction.

The transfer function formulation developed in the previous section is applied to synthesize the stepped shell. For the i th subsystem (shell segment) in Fig. 2, its response is expressed by

$$\eta_{i,n}(x, s) = e^{F_{i,n}(s)x} \left[\int_0^x e^{-F_{i,n}(s)\xi} \tilde{f}_{i,n}(\xi, s) d\xi + \eta_{i,n}(0, s) \right] \quad (18)$$

where x is a local dimensionless coordinate, the subscript n ($n = 1, 2, \dots$) is the circumferential wave number, and the subscript i ($1 \leq i \leq n_s$) indicates the i th subsystem. At the left and right ends of the stepped shell, $\eta_{1,n}$ and $\eta_{n_s,n}$ must satisfy the boundary condition

$$M_n(s) \eta_{1,n}(0, s) + N_n(s) \eta_{n_s,n}(1, s) = \gamma_n(s) \quad (19)$$

The shell is assembled from the n_s subsystems by imposing displacement continuity and force balance at the interconnecting boundaries of the shell segments. Two synthesis techniques are proposed: the connection matrix method and the nodal displacement method.

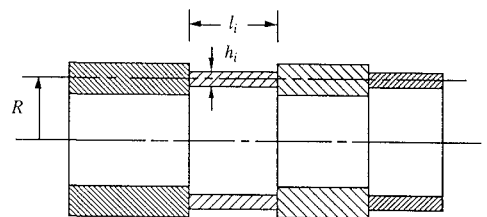


Fig. 2 Stepped cylindrical shell.

A. Connection Matrix Method

At the i th connecting boundary, the matching conditions for the two adjacent subsystems in general can be written as

$$R_{i,n}\eta_{i,n}(1,s) - R_{i+1,n}\eta_{i+1,n}(0,s) = \pi_{i,n}(s) \quad (20)$$

where $R_{i,n}$ and $R_{i+1,n}$ shall be called the connection matrices, and $\pi_{i,n}(s)$ counts for displacement and/or internal force jump due to the concentrated forces applied at the boundary. By Eqs. (18) and (19)

$$\begin{aligned} \eta_{i,n}(0,s) &= e^{-F_{i,n}(s)} R_{i,n}^{-1} [R_{i+1,n}\eta_{i+1,n}(0,s) + \pi_{i,n}(s)] \\ &- \int_0^1 e^{-F_{i,n}(s)\xi} f_{i,n}(\xi,s) d\xi \end{aligned} \quad (21)$$

Apply the previous formula recurrently to get

$$\eta_{1,n}(0,s) = P_{n_s}(s)\eta_{n_s,n}(0,s) + \bar{\pi}_n(s) - \bar{f}_n(s) \quad (22)$$

where

$$P_{n_s}(s) = \prod_{i=1}^{n_s-1} e^{-F_{i,n}(s)} R_{i,n}^{-1} R_{i+1,n} \quad (23a)$$

$$\bar{\pi}_n(s) = \sum_{i=1}^{n_s-1} \left[\prod_{j=1}^{i-1} e^{-F_{j,n}(s)} R_{j,n}^{-1} R_{j+1,n} \right] e^{-F_{i,n}(s)} R_{i,n}^{-1} \pi_{i,n}(s) \quad (23b)$$

$$\bar{f}_n(s) = \sum_{i=1}^{n_s-1} \left[\prod_{j=1}^{i-1} e^{-F_{j,n}(s)} R_{j,n}^{-1} R_{j+1,n} \right] \int_0^1 e^{-F_{i,n}(s)\xi} f_{i,n}(\xi,s) d\xi \quad (23c)$$

Substituting Eq. (22) into Eq. (19) yields

$$\bar{M}_n(s)\eta_{n_s,n}(0,s) + N_n(s)\eta_{n_s,n}(1,s) = \bar{\gamma}_n(s) + M_n(s)\bar{f}_n(s) \quad (24)$$

where

$$\bar{M}_n(s) = M_n(s)P_{n_s}(s), \quad \bar{\gamma}_n(s) = \gamma_n(s) - M_n(s)\bar{\pi}_n(s)$$

From Eqs. (18) and (24), it is found that

$$\begin{aligned} \eta_{n_s,n}(0,s) &= [\bar{M}_n(s) + N_n(s)e^{F_{n_s,n}(s)}]^{-1} \times \left[\bar{\gamma}_n + M_n(s)\bar{f}_n(s) \right. \\ &\left. - N_n(s)e^{F_{n_s,n}(s)} \int_0^1 e^{-F_{n_s,n}(s)\xi} f_{n_s,n}(\xi,s) d\xi \right] \end{aligned} \quad (25)$$

Finally, plugging Eq. (25) into Eq. (21), we arrive at

$$\begin{aligned} \eta_{i,n}(0,s) &= \left[\prod_{k=i}^{n_s-1} e^{-F_{k,n}(s)} R_{k,n}^{-1} R_{k+1,n} \right] \eta_{n_s,n}(0,s) \\ &+ \sum_{k=i}^{n_s-1} \left[\prod_{j=i}^{k-1} e^{-F_{j,n}(s)} R_{j,n}^{-1} R_{j+1,n} \right] e^{-F_{k,n}(s)} R_{k,n}^{-1} \pi_{k,n}(s) \\ &- \sum_{k=i}^{n_s-1} \left[\prod_{j=i}^{k-1} e^{-F_{j,n}(s)} R_{j,n}^{-1} R_{j+1,n} \right] \int_0^1 e^{-F_{k,n}(s)\xi} f_{k,n}(\xi,s) d\xi \end{aligned} \quad (26)$$

Hence, with $\eta_{i,n}(0,s)$ given in Eq. (26), the response $\eta_{i,n}(x,s)$ of each subsystem is completely determined by Eq. (18).

The eigenvalue problem (for both free vibration and buckling) of the stepped shell can be formulated by letting $\bar{\gamma}_n(s)$ and $\bar{f}_n(s)$ in Eqs. (18) and (24) be zero, leading to the characteristic equation

$$\det[\bar{M}_n(s)P_{n_s}(s) + N_n(s)e^{F_{n_s,n}(s)}] = 0 \quad (27)$$

With the eigenvalues calculated from Eq. (27), the mode shapes of each shell segment can be evaluated by Eqs. (15).

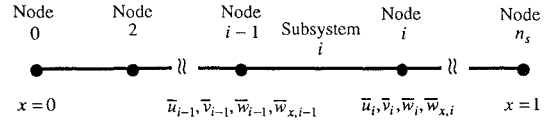


Fig. 3 Nodes and nodal displacements of the stepped shell.

B. Nodal Displacement Method

In this method, the finite element concept is introduced. To this end, the interconnecting boundaries between the adjacent subsystems (shell segments) shall be called nodes and denoted by $0, 1, 2, \dots, n_s$; see Fig. 3. For the i th subsystem, its left and right nodes are $i-1$ and i , respectively. The displacements at node i are \bar{u}_i, \bar{v}_i , and \bar{w}_i , the three displacements in the x, θ , and z directions, and $\bar{w}_{x,i}$, the slope of the transverse displacement in the x direction, respectively.

Define

$$\begin{aligned} u_i &= \begin{Bmatrix} \bar{u}_i \\ \bar{v}_i \\ \bar{w}_i \\ \bar{w}_{x,i} \end{Bmatrix}, \quad \begin{Bmatrix} f_{i,1} \\ f_{i,2} \end{Bmatrix} = \int_0^1 e^{-F_{i,n}(s)\xi} \bar{f}_{i,n}(\xi,s) d\xi \\ \begin{bmatrix} F_{i,11} & F_{i,12} \\ F_{i,21} & F_{i,22} \end{bmatrix} &= e^{F_{i,n}(s)} \end{aligned} \quad (28)$$

By letting $x=0$ and 1 in Eq. (18) and making use of Eq. (28), the state-space vector $\eta_{i,n}(0,s)$ is expressed by the nodal displacements:

$$\begin{aligned} \eta_{i,n}(0,s) &= \begin{bmatrix} I_{4 \times 4} & 0_{4 \times 4} \\ -F_{i,12}^{-1}F_{i,11} & F_{i,12}^{-1} \end{bmatrix} \begin{Bmatrix} u_{i-1} \\ u_i \end{Bmatrix} \\ &- \begin{bmatrix} 0_{4 \times 4} & 0_{4 \times 4} \\ -F_{i,12}^{-1}F_{i,11} & -F_{i,12}^{-1} \end{bmatrix} \begin{Bmatrix} f_{i,1} \\ f_{i,2} \end{Bmatrix} \end{aligned} \quad (29)$$

The vector of the internal forces, $\sigma_{i,n}(x,s)$, is related to the state-space vector $\eta_{i,n}(x,s)$ by

$$\sigma_{i,n}(x,s) = \bar{K}_{i,n}(s)\eta_{i,n}(x,s) \quad (30)$$

where $\bar{K}_{i,n}(s) \in C^{8 \times 8}$ is a constitutive matrix. Force balance at node i reads

$$\sigma_{i,n}(1,s) + \sigma_{i+1,n}(0,s) = q_{i,n}(s) \quad (31)$$

where $\sigma_{i,n}(1,s)$ and $\sigma_{i+1,n}(0,s)$ represent the internal forces at node i applied by the i th and $(i+1)$ th subsystems, respectively, and $q_{i,n}(s)$ is the vector of the external forces at node i . By Eqs. (18) and (28–31), it is found that

$$K_{i,n} \begin{Bmatrix} u_{i-1} \\ u_i \\ u_{i+1} \end{Bmatrix} = Q_{i,n} \quad (32)$$

where the stiffness matrix

$$\begin{aligned} K_{i,n} &= \bar{K}_{i,n} \begin{bmatrix} 0_{4 \times 4} & I_{4 \times 4} & 0_{4 \times 4} \\ F_{i,21} - F_{i,22}F_{i+1,12}^{-1}F_{i+1,11} & F_{i,22}^{-1}F_{i+1,12} & 0_{4 \times 4} \end{bmatrix} \\ &+ \bar{K}_{i+1,n} \begin{bmatrix} 0_{4 \times 4} & 0_{4 \times 4} & I_{4 \times 4} \\ 0_{4 \times 4} & -F_{i+1,12}^{-1}F_{i+1,11} & F_{i+1,12}^{-1}F_{i+1,11} \end{bmatrix} \end{aligned}$$

and the nodal force vector

$$\begin{aligned} Q_{i,n} &= q_{i,n} + \bar{K}_{i,n} \begin{bmatrix} 0_{4 \times 4} \\ F_{i,21} - F_{i,22}F_{i+1,12}^{-1}F_{i+1,11} \end{bmatrix} f_{i,1} \\ &+ \bar{K}_{i+1,n} \begin{bmatrix} I_{4 \times 4} \\ -F_{i+1,12}^{-1}F_{i+1,11} \end{bmatrix} f_{i+1,1} \end{aligned}$$

The boundary conditions of the stepped shell are substituted by plugging Eq. (29) into Eq. (19)

$$M_n \begin{bmatrix} I_{4 \times 4} & 0_{4 \times 4} \\ -F_{1,12}^{-1} F_{1,11} & F_{1,12}^{-1} \end{bmatrix} \begin{Bmatrix} u_0 \\ u_1 \end{Bmatrix} + N_n \begin{bmatrix} I_{4 \times 4} & 0_{4 \times 4} \\ -F_{n_s,12}^{-1} F_{n_s,11} & F_{n_s,12}^{-1} \end{bmatrix} \begin{Bmatrix} u_{n_s-1} \\ u_{n_s} \end{Bmatrix} = Q_{0,n} + Q_{n_s,n} \quad (33)$$

where

$$Q_{0,n} = M_n \begin{bmatrix} F_{1,12}^{-1} F_{1,11} & 0_{4 \times 4} \\ 0_{4 \times 4} & I_{4 \times 4} \end{bmatrix} \begin{Bmatrix} f_{1,1} \\ f_{1,2} \end{Bmatrix} + \gamma_{n,1}(s) \\ Q_{n_s,n} = -N_n \begin{bmatrix} I_{4 \times 4} \\ -F_{n_s,12}^{-1} F_{n_s,11} \end{bmatrix} f_{n_s,1} + \gamma_{n,2}, \quad \gamma_n = \begin{Bmatrix} \gamma_{n,1} \\ \gamma_{n,2} \end{Bmatrix}$$

Applying Eq. (32) to all nodes and combining the boundary condition (33) yield a global dynamic equilibrium equation

$$K_n(s)u(s) = Q_n(s) \quad (34)$$

where the subscript n is the shell circumferential wave number, the nodal displacement vector $u(s) = \{u_1^T \dots u_n^T\}^T$, the nodal force vector $Q(s) = \{Q_{0,n}^T \dots Q_{n_s,n}^T\}^T$, and the global dynamic stiffness matrix K_n is constructed in the same way as in the finite element method. Solve Eq. (34) for the node displacements and substitute the result back into Eqs. (18) and (29) to give $\eta_{i,n}(x, s)$. As such, the response of the stepped shell in every segment can be determined by Eq. (13).

The eigenvalue problem of the stepped shell becomes ($Q_n = 0$)

$$K_n(s)u(s) = 0 \quad (35)$$

The eigenvalues are determined from $\det K_n(\omega) = 0$. For an eigenvalue ω , its corresponding eigenfunction is obtained in two steps: 1) determine the nontrivial solution $u(\omega)$ from $K_n(\omega)u(\omega) = 0$, and 2) substitute $u(\omega)$ into Eqs. (29) and (18) to estimate $\eta_{i,n}(x, \omega)$.

IV. Application to Donnell–Mushtari Shell

A. Equations of Motion

The proposed transfer function method is applied to the Donnell–Mushtari model of cylindrical shells. The nondimensional equations of motion^{19,20} are

$$\frac{1}{\gamma_1^2} \frac{\partial^2 u}{\partial x^2} + \frac{1}{2}(1 - \mu) \frac{\partial^2 u}{\partial \theta^2} + \frac{1 + \mu}{2\gamma_1} \frac{\partial^2 v}{\partial x \partial \theta} - \frac{\mu}{\gamma_1} \frac{\partial w}{\partial x} = \bar{\rho} \frac{\partial^2 u}{\partial t^2} - \bar{q}_x \quad (36a)$$

$$\frac{1 + \mu}{2\gamma_1} \frac{\partial^2 u}{\partial x \partial \theta} + \frac{1 - \mu}{2\gamma_1^2} \frac{\partial^2 v}{\partial x^2} + \frac{\partial^2 v}{\partial \theta^2} - \frac{\partial w}{\partial \theta} = \bar{\rho} \frac{\partial^2 v}{\partial t^2} - \bar{q}_\theta \quad (36b)$$

$$\frac{\mu}{\gamma_1} \frac{\partial u}{\partial x} + \frac{\partial v}{\partial \theta} - w - k \left(\frac{1}{\gamma_1^4} \frac{\partial^4 w}{\partial x^4} + \frac{2}{\gamma_1^2} \frac{\partial^4 w}{\partial x^2 \partial \theta^2} + \frac{\partial^4 w}{\partial \theta^4} \right) + \frac{1}{J} \left(N_{x0} \frac{\partial^2 w}{\gamma_1^2 \partial x^2} + 2N_{x\theta 0} \frac{\partial^2 w}{\gamma_1 \partial x \partial \theta} + N_{\theta 0} \frac{\partial^2 w}{\partial \theta^2} \right) = \bar{\rho} \frac{\partial^2 w}{\partial t^2} - \bar{q}_z \quad (36c)$$

with

$$(u, v, w) = \frac{1}{h}(u_0, v_0, w_0)$$

$$(\bar{q}_x, \bar{q}_\theta, \bar{q}_z) = \frac{(1 - \mu^2)R^2}{Eh^2}(q_x, q_\theta, q_z) \quad \bar{\rho} = \frac{\rho(1 - \mu^2)R^2}{E}$$

$$\gamma_1 = \frac{L}{R}, \quad J = \frac{Eh}{1 - \mu^2}, \quad k = \frac{1}{12} \left(\frac{h}{R} \right)^2$$

Here u_0, v_0 , and w_0 are the displacements of the shell middle surface in the coordinate directions x, θ , and z , respectively; R, L , and h are the radius, length, and thickness of the shell, respectively; E and μ are Young's modulus and Poisson's ratio; ρ is the density per unit shell surface; $N_{x0}, N_{\theta 0}$, and $N_{x\theta 0}$ are the membrane stresses; and q_x, q_θ , and q_z are the loads on the shell.

There are four pairs of boundary conditions:

Condition 1:

$$u(x_i, \theta, t) = \bar{u}_i(\theta, t) \quad \text{or}$$

$$\frac{E}{1 - \mu^2} \frac{h^2}{R} \left[\frac{1}{\gamma_1} u_{,x} + \mu(v_{,\theta} - w) \right]_{x=x_i} = \bar{N}_{xi}(\theta, t) \quad (37a)$$

Condition 2:

$$v(x_i, \theta, t) = \bar{v}_i(\theta, t) \quad \text{or}$$

$$\frac{E}{2(1 + \mu)} \frac{h^2}{R} \left(u_{,\theta} + \frac{1}{\gamma_1} v_{,x} + \frac{2k}{\gamma_1} w_{,x\theta} \right)_{x=x_i} = \bar{N}_{x\theta i}^e(\theta, t) \quad (37b)$$

Condition 3:

$$w(x_i, \theta, t) = \bar{w}_i(\theta, t) \quad \text{or}$$

$$-\frac{E}{12(1 - \mu^2)} \frac{h^4}{R^3} \left[\frac{1}{\gamma_1^3} w_{,xxx} + \frac{2 - \mu}{\gamma_1} w_{,x\theta\theta} \right]_{x=x_i} = \bar{Q}_{x\theta i}^e(\theta, t) \quad (37c)$$

Condition 4:

$$w_{,x}|_{x=x_i} = \bar{w}_{x,i}(\theta, t) \quad \text{or}$$

$$-\frac{E}{12(1 - \mu^2)} \frac{h^4}{R^2} \left(\frac{1}{\gamma_1^2} w_{,xx} + \mu w_{,\theta\theta} \right)_{x=x_i} = \bar{M}_i(\theta, t) \quad (37d)$$

where $x_i = 0$ and 1 for $i = 1$ and 2 , for the left and right boundaries of the shell, respectively, and $u_{,x} = \partial u / \partial x$, etc.

B. Transfer Function Formulation

Although the transfer function method developed is valid for arbitrary disturbances, for the demonstrative purpose, we assume that all disturbances are symmetric with respect to $\theta = 0$. Thus, the Fourier expansions of the displacements and loads become

$$\begin{Bmatrix} u \\ v \\ w \end{Bmatrix} = \sum_{n=0}^{\infty} \begin{Bmatrix} u_n(x, t) \cos n\theta \\ v_n(x, t) \sin n\theta \\ w_n(x, t) \cos n\theta \end{Bmatrix} \quad (38) \\ \begin{Bmatrix} \bar{q}_x \\ \bar{q}_\theta \\ \bar{q}_z \end{Bmatrix} = \sum_{n=0}^{\infty} \begin{Bmatrix} q_{xn}(x, t) \cos n\theta \\ q_{\theta n}(x, t) \sin n\theta \\ q_{zn}(x, t) \cos n\theta \end{Bmatrix}$$

The η_n, F_n , and \bar{f}_n in Eq. (10a) have the form

$$\eta_n(x, s) = \left(\bar{u}_n \frac{\partial \bar{u}_n}{\partial x} \quad \bar{v}_n \frac{\partial \bar{v}_n}{\partial x} \quad \bar{w}_n \frac{\partial \bar{w}_n}{\partial x} \quad \frac{\partial^2 \bar{w}_n}{\partial x^2} \quad \frac{\partial^3 \bar{w}_n}{\partial x^3} \right)^T \quad (39a)$$

$$F_n(s) = \begin{bmatrix} F_{11} & F_{12} \\ F_{21} & F_{22} \end{bmatrix} \in C^{8 \times 8} \quad (39b)$$

$$\bar{f}_n(x, s) + \bar{g}_n(x, s) = \begin{Bmatrix} 0 & -\gamma_1^2 [\bar{\rho}(s u_{0,n} + \dot{u}_{0,n}) + \bar{q}_{xn}] & 0 & 0 & 0 \\ -\frac{2\gamma_1^2}{1 - \mu} [\bar{\rho}(s v_{0,n} + \dot{v}_{0,n}) + \bar{q}_{\theta n}] & 0 & 0 & 0 & 0 \\ \frac{\gamma_1^4}{k} [\bar{\rho}(s w_{0,n} + \dot{w}_{0,n}) + \bar{q}_{zn}] \end{Bmatrix}^T \quad (39c)$$

where the tilde denotes Laplace transformation, the over-dot stands for time derivative, and

$$F_{11} = \begin{bmatrix} 0 & 1 & 0 & 0 \\ \gamma_1^2 \left(\frac{1-\mu}{2} n^2 + s^2 \bar{\rho} \right) & 0 & 0 & -\frac{1+\mu}{2} n \gamma_1 \\ 0 & 0 & 0 & 1 \\ 0 & \gamma_1 n \frac{1+\mu}{1-\mu} & \frac{2n^2 \gamma_1^2}{1-\mu} + \frac{2\bar{\rho} s^2 \gamma_1^2}{1-\mu} & 0 \end{bmatrix}$$

$$F_{12} = \begin{bmatrix} 0 & 0 & 0 & 0 \\ 0 & \mu \gamma_1 & 0 & 0 \\ 0 & 0 & 0 & 0 \\ -\frac{2n \gamma_1^2}{1-\mu} & 0 & 0 & 0 \end{bmatrix}, \quad F_{21} = \begin{bmatrix} 0 & 0 & 0 & 0 \\ 0 & 0 & 0 & 0 \\ 0 & 0 & 0 & 0 \\ 0 & \gamma_1^3 \frac{\mu}{k} & \frac{n \gamma_1^4}{k} & 0 \end{bmatrix}$$

$$F_{22} = \begin{bmatrix} 0 & 1 & 0 & 0 \\ 0 & 0 & 1 & 0 \\ 0 & 0 & 0 & 1 \\ -\gamma_1^4 \left(\frac{1}{k} + n^4 + \frac{\bar{\rho}}{k} s^2 \right) - \frac{n^2 \gamma_1^4 N_{\theta 0}}{kJ} & -\frac{2n \gamma_1^3 N_{x\theta 0}}{kJ} & 2n^2 \gamma_1^2 + \frac{\gamma_1^2 N_{x0}}{kJ} & 0 \end{bmatrix}$$

Similarly, Fourier expansions of the boundary disturbances in Eq. (37) are

$$\begin{aligned} \bar{u}_i(\theta, t) &= \sum_{n=0}^{\infty} \bar{u}_n^i(t) \cos n\theta \\ \bar{v}_i(\theta, t) &= \sum_{n=1}^{\infty} \bar{v}_n^i(t) \sin n\theta \end{aligned} \quad (40a)$$

$$\begin{aligned} \bar{w}_i(\theta, t) &= \sum_{n=0}^{\infty} \bar{w}_n^i(t) \cos n\theta \\ \bar{w}_{x,i}(\theta, t) &= \sum_{n=0}^{\infty} \bar{w}_{x,n}^i(t) \cos n\theta \end{aligned} \quad (40b)$$

$$\begin{aligned} \bar{N}_{xi}(\theta, t) &= \frac{(1-\mu^2)R}{Eh^2} \sum_{n=0}^{\infty} \bar{N}_{x,n}^i(t) \cos n\theta \\ \bar{N}_{x\theta i}^e(\theta, t) &= \frac{2(1+\mu)R}{Eh^2} \sum_{n=1}^{\infty} \bar{N}_{x\theta,n}^{ei}(t) \sin n\theta \end{aligned} \quad (40c)$$

$$\begin{aligned} \bar{Q}_{xi}^e(\theta, t) &= -\frac{12(1-\mu^2)R^3}{Eh^4} \sum_{n=0}^{\infty} \bar{Q}_{x,n}^{ei}(t) \cos n\theta \\ \bar{M}_i(\theta, t) &= -\frac{12(1-\mu^2)R^2}{Eh^4} \sum_{n=0}^{\infty} \bar{M}_x^i(t) \cos n\theta \end{aligned} \quad (40d)$$

By Eqs. (37), (38), and (40), the M_n , N_n , and γ_n in Eq. (10b) are obtained as

$$M_n = \begin{bmatrix} B_1 L_n \\ 0_{4 \times 8} \end{bmatrix}, \quad N_n = \begin{bmatrix} 0_{4 \times 8} \\ B_2 L_n \end{bmatrix} \quad (41a)$$

$$\gamma_n(s) = \begin{Bmatrix} \tilde{\gamma}_n^1 \\ \tilde{\gamma}_n^2 \end{Bmatrix} \quad (41b)$$

where

$$\begin{aligned} \tilde{\gamma}_n^i &= \begin{bmatrix} \bar{u}_n^i(s) & \frac{1-\mu^2}{Eh^2} R \bar{N}_{x,n}^i(s) & \bar{v}_n^i(s) & \frac{2(1+\mu)}{Eh^2} R \bar{N}_{x\theta,n}^i(s) \\ \bar{w}_n^i(s) & -\frac{12(1-\mu^2)}{Eh^4} R^3 \bar{Q}_{x,n}^i(s) & \bar{w}_n^i(s) & -\frac{12(1-\mu^2)R^2}{Eh^4} \bar{M}_{x,n}^i(s) \end{bmatrix}^T \end{aligned}$$

$L_n =$

$$\begin{bmatrix} 1 & 0 & 0 & 0 & 0 & 0 & 0 & 0 \\ 0 & 1/\gamma_1 & n\mu & 0 & -\mu & 0 & 0 & 0 \\ 0 & 0 & 1 & 0 & 0 & 0 & 0 & 0 \\ -n & 0 & 0 & 1/\gamma_1 & 0 & -kn/(6\gamma_1) & 0 & 0 \\ 0 & 0 & 0 & 0 & 1 & 0 & 0 & 0 \\ 0 & 0 & 0 & 0 & 0 & -(2-\mu)n^2/\gamma_1 & 0 & 1/\gamma_1^3 \\ 0 & 0 & 0 & 0 & 0 & 1 & 0 & 0 \\ 0 & 0 & 0 & 0 & -\mu n^2 & 0 & 1/\gamma_1^2 & 0 \end{bmatrix}$$

with $i = 1$ and 2 for the left and right boundaries of the shell, respectively, and B_1 and B_2 are 4×8 matrices containing Kronecker deltas δ_{ij} .

With the state-space matrix F_n and the boundary matrices M_n and N_n derived, the transfer functions of the shell can be evaluated by Eq. (12), and the response of the shell subject to various external excitations are boundary conditions can be determined by Eq. (11).

C. Connection Matrix

The connection matrix is needed when stepped cylindrical shells are analyzed using the connection matrix method discussed in Sec. III. Without loss of generality, assume that all segments of a stepped shell are completely bonded such that the displacements and internal forces are continuous at the interconnecting boundaries of the shell segments. Under the assumption, the connection matrix

R_i is found as

$$R_{i,n} = \begin{bmatrix} \bar{h}_i & 0 & 0 & 0 & 0 & 0 & 0 & 0 \\ 0 & 0 & \bar{h}_i & 0 & 0 & 0 & 0 & 0 \\ 0 & 0 & 0 & 0 & \bar{h}_i & 0 & 0 & 0 \\ 0 & 0 & 0 & 0 & 0 & \bar{h}_i/\bar{L}_i & 0 & 0 \\ 0 & \bar{k}_{i,1}\bar{\gamma}_2 & \bar{k}_{i,1}\bar{\mu}_i n & 0 & -\bar{k}_{i,1}\bar{\mu}_i & 0 & 0 & 0 \\ -\bar{k}_{i,2}n & 0 & 0 & \bar{k}_{i,2}\bar{\gamma}_2 & 0 & -\bar{k}_{i,2}n\bar{h}_i^2\bar{\gamma}_2/(6R^2) & 0 & 0 \\ 0 & 0 & 0 & 0 & 0 & \bar{k}_{i,3}n^2(2-\bar{\mu}_i)\bar{\gamma}_2 & 0 & -\bar{k}_{i,3}\bar{\gamma}_2^3 \\ 0 & 0 & 0 & 0 & 0 & \bar{k}_{i,3}\bar{\mu}_i n^2 R & -\bar{k}_{i,3}\bar{\gamma}_2^3 R & 0 \end{bmatrix} \quad (42)$$

where

$$\bar{k}_{i,1} = \frac{\bar{E}_i \bar{h}_i^2}{(1-\bar{\mu}_i^2)R}, \quad \bar{k}_{i,2} = \frac{\bar{E}_i \bar{h}_i^2}{2(1+\bar{\mu}_i)R}$$

$$\bar{k}_{i,3} = \frac{\bar{E}_i \bar{h}_i^4}{12(1-\bar{\mu}_i^2)R^3}, \quad \bar{\gamma}_i = \frac{R}{\bar{L}_i}$$

and where \bar{E}_i , $\bar{\mu}_i$, \bar{L}_i , and h_i are Young's module, Poisson's ratio, length, and height of the i th shell, respectively.

V. Numerical Results

The numerical examples are based on the Donnell–Mushtari shell model [Eqs. (36)]. Having determined the state-space matrices and the connection matrix in Sec. IV, we are ready to address various static and dynamic problems for homogeneous and stepped shells.

A. Free Vibration of a Homogenous Shell

Consider the following dimensionless geometry and material parameters:

$$E = 100, \quad \mu = 0.3, \quad R = L = 100$$

$$h = 1, \quad \rho = 1 \quad (43)$$

Simply supported boundary conditions

$$v = 0, \quad w = 0, \quad N_x = 0, \quad M_x = 0 \quad (44)$$

are assumed at the both ends of the shell. In this case, the classical boundary-value approach can also give the exact characteristic equation, which is¹⁹

$$\det(A + \omega^2 I) = 0 \quad (45)$$

with

$$A = \frac{E}{\rho(1-\mu^2)R^2} \begin{bmatrix} -\left(\frac{m^2\pi^2}{\gamma_1^2} + \frac{1-\mu}{2}n^2\right) & \frac{1+\mu}{2\gamma_1}nm\pi & -\frac{\mu}{\gamma_1}m\pi \\ \frac{1+\mu}{2\gamma_1}nm\pi & -\left(\frac{1-\mu}{2\gamma_1^2}m^2\pi^2 + n^2\right) & n \\ -\frac{\mu}{\gamma_1}m\pi & n & -1-k\left(\frac{m^4\pi^4}{\gamma_1^4} + \frac{2n^2m^2\pi^2}{\gamma_1^2} + n^4\right) \end{bmatrix}$$

Shown in Table 1 are the first 12 natural frequencies ω_{mn} of the cylindrical shell, where the subscript m is the shell wave number along its longitudinal direction x . The circumferential wave number $n = 7$ is chosen such that the natural frequency ω_{17} is the fundamental (lowest) frequency of the shell. Both the transfer function method, Eq. (14), and the boundary-value approach, Eq. (45), have been used in the calculation, and they produce almost the same result.

B. Buckling of a Homogenous Shell

The shell is under both axial compression N_{x0} and hydrostatic pressure $N_{\theta 0}$; see Eq. (36c). Consider the same shell parameters as given in Eq. (43) and the simply supported boundary conditions of Eq. (44). Neglect the prebuckling effects. The buckling loads, calculated by the transfer function method, Eq. (14), are shown in Tables 2 and 3 for two cases: the shell under axial compression and hydrostatic pressure, respectively. Here the circumferential wave number $n = 6$ ($n = 8$) is chosen to reach the lowest buckling load N_{16} (N_{18}) in the axial compression (hydrostatic pressure) case. The transfer function method is compared with the boundary-value approach, which gives exact estimation of the buckling loads by²¹

$$\det \begin{bmatrix} -\left(\frac{m^2\pi^2}{\gamma_1^2} + \frac{1-\mu}{2}n^2\right) & \frac{1+\mu}{2\gamma_1}nm\pi & -\frac{\mu}{\gamma_1}m\pi \\ \frac{1+\mu}{2\gamma_1}nm\pi & -\left(\frac{1-\mu}{2\gamma_1^2}m^2\pi^2 + n^2\right) & n \\ -\frac{\mu}{\gamma_1}m\pi & n & \phi \end{bmatrix} = 0 \quad (46)$$

where

$$\phi = -1 - k\left(\frac{m^4\pi^4}{\gamma_1^4} + \frac{2n^2m^2\pi^2}{\gamma_1^2} + n^4\right)$$

$$- \frac{1}{J}\left(\frac{m^2\pi^2 N_{x0}}{\gamma_1^2} + n^2 N_{\theta 0}\right)$$

C. Free Vibration of a Stepped Shell

Consider a stepped shell of three shell segments. The geometry and material parameters of the shell segment are as follows:

Subsystem 1:

$$l_1 = 40, \quad h_1 = 1, \quad E_1 = 100, \quad \mu_1 = 0.3$$

Subsystem 2:

$$l_2 = 20, \quad h_2 = 3, \quad E_2 = 100, \quad \mu_2 = 0.3$$

Subsystem 3:

$$l_3 = 40, \quad h_3 = 1, \quad E_3 = 100, \quad \mu_3 = 0.3$$

Table 1 Natural frequencies ω_{mn} of the cylindrical shell (simply supported, $n = 7$)

Mode no. m of ω_{m7}	Transfer function method	Boundary-value approach
1	0.0242	0.0242
2	0.0516	0.0516
3	0.0764	0.0764
4	0.0985	0.0985
5	0.1222	0.1222
6	0.1505	0.1505
7	0.1849	0.1849
8	0.2259	0.2259
9	0.2743	0.2743
10	0.3276	0.3276
11	0.3878	0.3882
12	0.4375	0.4341

Table 2 Buckling loads N_{mn} of the shell under axial compression (simply supported, $n = 6$)

Mode no. m of N_{m6}	Transfer function method	Boundary-value approach
1	0.6053	0.6054
2	0.6267	0.6267
3	0.6380	0.6380
4	0.6643	0.6643
5	0.6904	0.6904
6	0.7307	0.7307
7	0.7880	0.7880
8	0.8251	0.8251
9	0.9140	0.9140
10	1.0653	1.0653
11	1.2394	1.2394
12	1.4352	1.4352

Table 3 Buckling loads N_{mn} of the shell under hydrostatic pressure (simply supported, $n = 8$)

Mode no. m of N_{m8}	Transfer function method	Boundary-value approach
1	0.1060	0.1060
2	0.3806	0.3806
3	0.8620	0.8620
4	1.4958	1.4958
5	2.3668	2.3668
6	3.6376	3.6376
7	5.5094	5.5094
8	8.2127	8.2127
9	12.0068	12.0069
10	17.1820	17.1821
11	24.0055	24.0599
12	32.4008	32.9939

Table 4 Natural frequencies ω_{mn} of the stepped shell (simply supported $n = 5$)

Mode no. m of ω_{m5}	Transfer function method	Finite element method
1	0.02944	0.02909
2	0.07115	0.07099
3	0.08471	0.08464
4	0.11111	0.11080
5	0.13660	0.13659
6	0.15720	0.15701
7	0.21960	0.21958
8	0.24255	0.24240
9	0.28263	0.28396
10	0.33358	0.33315
11	0.37058	0.37055
12	0.40638	0.42373

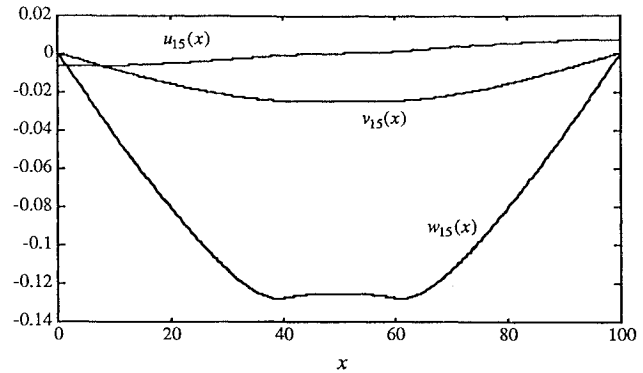


Fig. 4a The mode shapes of the shell (simply supported SS3): $\omega_{15} = 0.02944$.

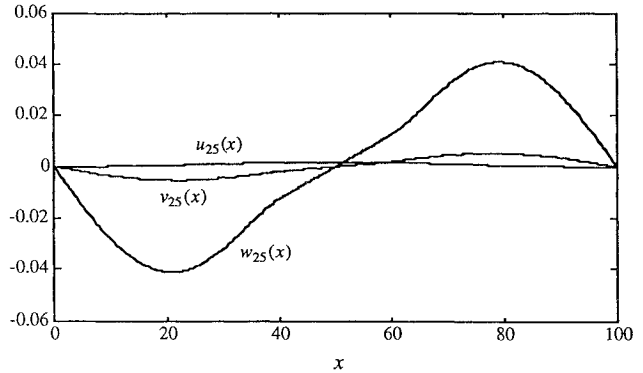


Fig. 4b The mode shapes of the shell (simply supported SS3): $\omega_{25} = 0.07115$.

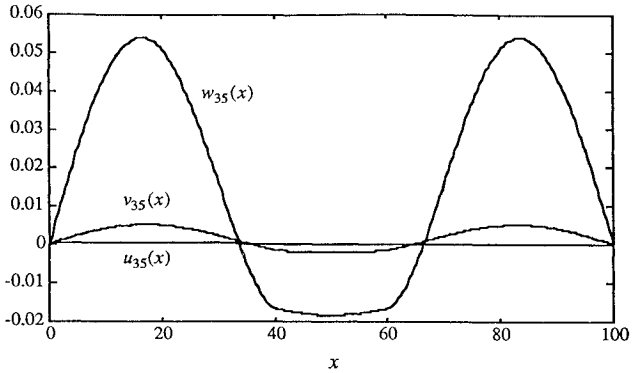


Fig. 4c The mode shapes of the shell (simply supported SS3): $\omega_{35} = 0.08471$.

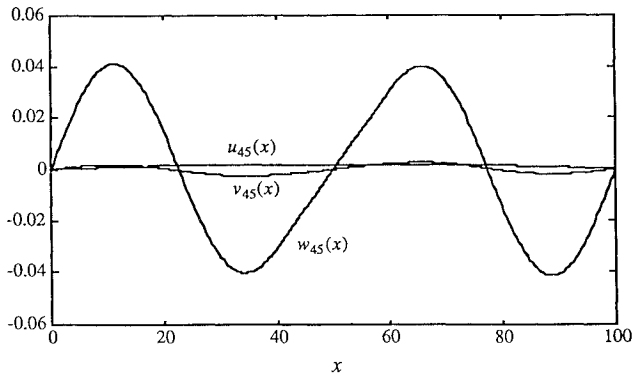


Fig. 4d The mode shapes of the shell (simply supported SS3): $\omega_{45} = 0.11111$.

Table 5 Natural frequencies ω_{mn} of the stepped cylindrical shell under various boundary conditions (m = longitudinal wave number, n = circumferential wave number)

m	SS1 ($n = 5$)	SS2 ($n = 2$)	SS4 ($n = 2$)	CC1 ($n = 5$)	CC2 ($n = 4$)	CC3 ($n = 5$)	CC4 ($n = 4$)	FF1 ($n = 2$)
1	0.03261	0.02081	0.02066	0.03343	0.02850	0.03030	0.02709	0.00216
2	0.07115	0.08137	0.03276	0.07447	0.06795	0.07115	0.06149	0.00381
3	0.08472	0.09374	0.09260	0.09046	0.08715	0.08471	0.08634	0.08557
4	0.11116	0.10885	0.10403	0.11869	0.11539	0.11114	0.11535	0.09953
5	0.13665	0.13630	0.10934	0.15241	0.15025	0.13662	0.15008	0.10482
6	0.15753	0.15088	0.13630	0.17342	0.16892	0.15743	0.16530	0.10737
7	0.21964	0.20934	0.15152	0.24489	0.24142	0.21962	0.19785	0.11803
8	0.24258	0.21327	0.21285	0.26996	0.26322	0.24257	0.24108	0.15312
9	0.32388	0.23286	0.22008	0.32390	0.26902	0.30005	0.26687	0.16913
10	0.33356	0.23643	0.23618	0.36426	0.35974	0.33356	0.34702	0.21901
11	0.37061	0.32527	0.31392	0.41544	0.40642	0.37061	0.35974	0.24046
12	0.41099	0.35410	0.32519	0.43032	0.43529	0.41099	0.40642	0.26512

The radius of the stepped shell $R = 100$. This is a shell of varying thickness. The transfer function synthesis of the stepped shell is based on the connection matrix method presented in Sec. III. To show the flexibility of the transfer function method, the following nine sets of boundary conditions are considered in the simulation:

Four sets of simple-simple boundary conditions:

$$\begin{aligned} \text{(SS1)} \quad w^{(1)}(0) = M_x^{(1)}(0) = u^{(1)}(0) = v^{(1)}(0) = w^{(3)}(1) \\ = M_x^{(3)}(1) = u^{(3)}(1) = v^{(3)}(1) = 0 \end{aligned} \quad (47a)$$

$$\begin{aligned} \text{(SS2)} \quad w^{(1)}(0) = M_x^{(1)}(0) = u^{(1)}(0) = N_{x\theta}^{(1)}(0) = w^{(3)}(1) \\ = M_x^{(3)}(1) = u^{(3)}(1) = N_{x\theta}^{(3)}(1) = 0 \end{aligned} \quad (47b)$$

$$\begin{aligned} \text{(SS3)} \quad w^{(1)}(0) = M_x^{(1)}(0) = N_x^{(1)}(0) = v^{(1)}(0) = w^{(3)}(1) \\ = M_x^{(3)}(1) = N_x^{(3)}(1) = v^{(3)}(1) = 0 \end{aligned} \quad (47c)$$

$$\begin{aligned} \text{(SS4)} \quad w^{(1)}(0) = M_x^{(1)}(0) = N_x^{(1)}(0) = N_{x\theta}^{(1)}(0) = w^{(3)}(1) \\ = M_x^{(3)}(1) = N_x^{(3)}(1) = N_{x\theta}^{(3)}(1) = 0 \end{aligned} \quad (47d)$$

Four sets of clamped-clamped boundary conditions:

$$\begin{aligned} \text{(CC1)} \quad w^{(1)}(0) = w_{,x}^{(1)}(0) = u^{(1)}(0) = v^{(1)}(0) = w^{(3)}(1) \\ = w_{,x}^{(3)}(1) = u^{(3)}(1) = v^{(3)}(1) = 0 \end{aligned} \quad (47e)$$

$$\begin{aligned} \text{(CC2)} \quad w^{(1)}(0) = w_{,x}^{(1)}(0) = u^{(1)}(0) = N_{x\theta}^{(1)}(0) = w^{(3)}(1) \\ = w_{,x}^{(3)}(1) = u^{(3)}(1) = N_{x\theta}^{(3)}(1) = 0 \end{aligned} \quad (47f)$$

$$\begin{aligned} \text{(CC3)} \quad w^{(1)}(0) = w_{,x}^{(1)}(0) = N_x^{(1)}(0) = v^{(1)}(0) = w^{(3)}(1) \\ = w_{,x}^{(3)}(1) = N_x^{(3)}(1) = v^{(3)}(1) = 0 \end{aligned} \quad (47g)$$

$$\begin{aligned} \text{(CC4)} \quad w^{(1)}(0) = w_{,x}^{(1)}(0) = N_x^{(1)}(0) = N_{x\theta}^{(1)}(0) = w^{(3)}(1) \\ = w_{,x}^{(3)}(1) = N_x^{(3)}(1) = N_{x\theta}^{(3)}(1) = 0 \end{aligned} \quad (47h)$$

One set of free-free boundary conditions:

$$\begin{aligned} \text{(FF1)} \quad Q_x^{(1)}(0) = M_x^{(1)}(0) = N_x^{(1)}(0) = N_{x\theta}^{(1)}(0) = Q_x^{(3)}(1) \\ = M_x^{(3)}(1) = N_x^{(3)}(1) = N_{x\theta}^{(3)}(1) = 0 \end{aligned} \quad (47i)$$

where the superscripts (1) and (3) designate the left and right shell segments, respectively.

The proposed transfer function method is first compared with the finite element method (FEM) since the exact results by other analytical methods are not available. Table 4 shows the first 12 lowest natural frequencies of the shell under the simply supported boundary conditions (SS3), where m and n are the longitudinal and circumferential wave numbers, respectively. Good agreement between the proposed method and FEM is seen. It is found that the fundamental frequency of the shell is ω_{15} . Figure 4 plot the mode shapes of the shell, where $u_{mn}(x)$, $v_{mn}(x)$, and $w_{mn}(x)$ are the eigenfunctions corresponding to the frequency ω_{mn} listed in Table 4.

The natural frequencies of the stepped shell under the other eight sets of boundary conditions are also calculated by the transfer function method, and they are presented in Table 5. Here the circumferential wave number n is selected so that ω_{1n} is the fundamental frequency of the shell under the specified boundary conditions. In treating each set of boundary conditions, the transfer function method simply changes the entries of the matrices M_n and N_n and does not need different derivations.

VI. Conclusions

A theoretical and numerical method has been developed for modeling and analysis of general cylindrical shells. Through the use of Fourier expansion and Laplace transform, an infinite set of decoupled ordinary differential equations are obtained. With a state-space technique, the solutions of those decoupled equations are then expressed by a compact matrix form, leading to the exact distributed transfer functions of the cylindrical shell. Based on the transfer functions, exact and closed-form solutions of various static and dynamic problems of cylindrical shells can be obtained. Because it is able to describe different shell models (with arbitrary boundary conditions and external loads) in an unified form, the proposed transfer function method is easy and efficient in computer programming for numerical simulation. Although the transfer function synthesis in this paper is limited to stepped cylindrical shells, the theoretical results obtained are readily extended to shells with continuously varying thickness and shells with stiffeners.¹⁸

Appendix

Denote the elements of a matrix $S \in C^{2N \times 2N}$ and a vector $U \in C^{2N}$ by $S(i, j)$ and $U(i)$, respectively. Denote the k th row of a matrix $S \in C^{2N \times 2N}$ by $S(k, *) \in C^{1 \times 2N}$. Let δ_i^j be the Kronecker delta. The $F_n(s)$, $\tilde{f}_n(x, s)$, and $\tilde{g}_n(x, s)$ in Eq. (10a) are expressed by the following:

$$F_n(i, j) = \delta_{i+1}^j \text{ for } i \neq j(n_k - 1), j = 1, 2 \text{ and } k = 1, 2, 3 \quad (\text{A1})$$

$$\begin{aligned} F_n(n_m - 1, *) = \frac{-1}{D_{mmn0}} \\ \times \{ \bar{D}_{m10} \quad 0 \quad \bar{D}_{m12} \quad 0 \quad \cdots \quad \bar{D}_{m1(n_1-2)} \quad 0 \quad 0 \quad \bar{D}_{m11} \quad 0 \quad \bar{D}_{m13} \quad 0 \quad \cdots \quad \bar{D}_{m1(n_1-1)} \\ \bar{D}_{m20} \quad 0 \quad \bar{D}_{m22} \quad 0 \quad \cdots \quad \bar{D}_{m2(n_2-2)} \quad 0 \quad 0 \quad \bar{D}_{m21} \quad 0 \quad \bar{D}_{m23} \quad 0 \quad \cdots \quad \bar{D}_{m2(n_2-1)} \\ \bar{D}_{m30} \quad 0 \quad \bar{D}_{m32} \quad 0 \quad \cdots \quad \bar{D}_{m3(n_3-2)} \quad 0 \quad 0 \quad \bar{D}_{m31} \quad 0 \quad \bar{D}_{m33} \quad 0 \quad \cdots \quad \bar{D}_{m3(n_3-1)} \} \end{aligned} \quad (\text{A2})$$

$$F_n(2(n_m - 1), *) = \frac{-1}{D_{mmn_k0}}$$

$$\times \{0 \quad \bar{d}_{m11} \quad 0 \quad \bar{d}_{m13} \quad 0 \quad \cdots \quad \bar{d}_{m1(n_1-1)} \quad \bar{d}_{m10} \quad 0 \quad \bar{d}_{m12} \quad 0 \quad \cdots \quad \bar{d}_{m1(n_1-2)} \quad 0$$

$$0 \quad \bar{d}_{m21} \quad 0 \quad \bar{d}_{m23} \quad 0 \quad \cdots \quad \bar{d}_{m2(n_2-1)} \quad \bar{d}_{m20} \quad 0 \quad \bar{d}_{m22} \quad 0 \quad \cdots \quad \bar{d}_{m2(n_2-2)} \quad 0$$

$$0 \quad \bar{d}_{m31} \quad 0 \quad \bar{d}_{m33} \quad 0 \quad \cdots \quad \bar{d}_{m3(n_3-1)} \quad \bar{d}_{m30} \quad 0 \quad \bar{d}_{m32} \quad 0 \quad \cdots \quad \bar{d}_{m3(n_3-2)} \quad 0\}$$

for $m = 1, 2, 3$;

$$\bar{D}_{mki} = \sum_{i=h}^{n_k-1} \bar{D}_{mki(i-h)}$$

$$\bar{D}_{mki(i-h)} = \begin{cases} (-1)^{\frac{h}{2}} D_{mki(i-h)}, & h = 0, 2, 4, \dots \\ (-1)^{\frac{h-1}{2}} D_{mki(i-h)}, & h = 1, 3, 5, \dots \end{cases} \quad (A3)$$

$$\bar{d}_{mki} = \sum_{i=h}^{n_k-1} \bar{d}_{mki(i-h)}$$

$$\bar{d}_{mki(i-h)} = \begin{cases} (-1)^{\frac{h}{2}} D_{mki(i-h)}, & h = 0, 2, 4, \dots \\ (-1)^{\frac{h-1}{2}} D_{mki(i-h)}, & h = 1, 3, 5, \dots \end{cases}$$

for $h = 0, 1, \dots, n_k-1$, and $k, m = 1, 2, 3$;

$$\tilde{f}_n(n_k - 1) = \frac{\tilde{f}_{1,n}^1}{D_{11n_k0}}$$

$$\tilde{f}_n(2n_k - 2) = \frac{\tilde{f}_{2,n}^1}{D_{11n_k0}} \quad \text{for } k = 1, 2, 3$$

$$\tilde{f}_n(j) = 0 \quad \text{for } j \neq i(n_k - 1), \quad i = 1, 2 \quad k = 1, 2, 3$$

$$\tilde{g}_n(n_k - 1) = \frac{\tilde{g}_{1,n}^1}{D_{11n_k0}}$$

$$\tilde{g}_n(2n_k - 2) = \frac{\tilde{g}_{2,n}^1}{D_{11n_k0}} \quad \text{for } k = 1, 2, 3$$

$$\tilde{g}_n(j) = 0 \quad \text{for } j \neq i(n_k - 1), \quad i = 1, 2, k = 1, 2, 3 \quad (A4)$$

Equations (9) are arranged such that the first n_b equations are for the left boundary of the shell ($x = 0$) and the last n_b equations are for the right $x = L$. As such, the boundary matrices in Eq. (10b) become

$$M_n(s) = \begin{bmatrix} I_{n_b \times n_b} & 0 \\ 0 & 0 \end{bmatrix} T_n, \quad N_n(s) = \begin{bmatrix} 0 & 0 \\ 0 & I_{n_b \times n_b} \end{bmatrix} T_n$$

where

$$T_n(2l - 1, *)$$

$$= \{\bar{T}_{l10} \quad 0 \quad \bar{T}_{l12} \quad 0 \cdots \bar{T}_{l1(n_1-2)} \quad 0 \quad 0 \quad \bar{T}_{l11} \quad 0 \quad \bar{T}_{l13} \quad 0 \cdots \bar{T}_{l1(n_1-1)} \quad \bar{T}_{l20} \quad 0 \quad \bar{T}_{l22} \quad 0 \cdots \bar{T}_{l2(n_2-2)} \quad 0 \quad 0 \quad \bar{T}_{l21} \quad 0 \quad \bar{T}_{l23} \quad 0 \cdots \bar{T}_{l2(n_2-1)} \quad \bar{T}_{l30} \quad 0 \quad \bar{T}_{l32} \quad 0 \cdots \bar{T}_{l3(n_3-2)} \quad 0 \quad 0 \quad \bar{T}_{l31} \quad 0 \quad \bar{T}_{l33} \quad 0 \cdots \bar{T}_{l3(n_3-1)}\}$$

$$T_n(2l, *)$$

$$= \{0 \quad \bar{t}_{l11} \quad 0 \quad \bar{t}_{l13} \quad 0 \cdots \bar{t}_{l1(n_1-1)} \quad \bar{t}_{l10} \quad 0 \quad \bar{t}_{l12} \quad 0 \cdots \bar{t}_{l1(n_1-2)} \quad 0 \quad \bar{t}_{l21} \quad 0 \quad \bar{t}_{l23} \quad 0 \cdots \bar{t}_{l2(n_2-1)} \quad \bar{t}_{l20} \quad 0 \quad \bar{t}_{l22} \quad 0 \cdots \bar{t}_{l2(n_2-2)} \quad 0 \quad \bar{t}_{l31} \quad 0 \quad \bar{t}_{l33} \quad 0 \cdots \bar{t}_{l3(n_3-1)} \quad \bar{t}_{l30} \quad 0 \quad \bar{t}_{l32} \quad 0 \cdots \bar{t}_{l3(n_3-2)} \quad 0\}$$

$$\bar{T}_{mki} = \sum_{i=h}^{n_k-1} T_{mki(i-h)}$$

$$T_{mki(i-h)} = \begin{cases} (-1)^{\frac{h}{2}} \beta_{mki(i-h)}, & \text{for } h = 0, 2, 4, \dots \\ (-1)^{\frac{h-1}{2}} \beta_{mki(i-h)}, & \text{for } h = 1, 3, 5, \dots \end{cases}$$

$$\bar{d}_{mki} = \sum_{i=h}^{n_k-1} t_{mki(i-h)}$$

$$t_{mki(i-h)} = \begin{cases} (-1)^{\frac{h}{2}} \beta_{mki(i-h)}, & \text{for } h = 0, 2, 4, \dots \\ (-1)^{\frac{h-1}{2}} \beta_{mki(i-h)}, & \text{for } h = 1, 3, 5, \dots \end{cases}$$

The boundary disturbance vector $\gamma_n(s)$ is given by

$$\gamma_n(s) = \{\tilde{\lambda}_{1,n}^1 \quad \tilde{\lambda}_{2,n}^1 \quad \tilde{\lambda}_{1,n}^2 \quad \tilde{\lambda}_{2,n}^2 \quad \cdots \quad \tilde{\lambda}_{1,n}^{n_b} \quad \tilde{\lambda}_{2,n}^{n_b}\}$$

Acknowledgments

This work was partially supported by the U.S. Army Research Office under Grant DAAL03-93-G-0066 with Gary L. Anderson as the technical monitor.

References

- Irie, T., Yamada, G., and Kudoh, Y., "Free Vibration of Point-Supported Circular Cylindrical Shell," *Journal of Acoustic Society of America*, Vol. 75, No. 4, 1984, pp. 1118-1123.
- Yamada, G., Irie, T., and Tsushima, M., "Vibration and Stability of Orthotropic Circular Cylindrical Shells Subjected to Axial Load," *Journal of Acoustic Society of America*, Vol. 75, No. 3, 1984, pp. 842-848.
- Sheinman, I., and Weissman, S., "Coupling Between Symmetric and Antisymmetric Modes in Shells and Revolution," *Journal of Composite Materials*, Vol. 21, No. 11, 1987, pp. 988-1007.
- Koga, T., "Effects of Boundary Conditions on the Free Vibrations of Circular Cylindrical Shells," *AIAA Journal*, Vol. 26, No. 11, 1988, pp. 1387-1394.
- Koga, T., and Morimatsu, S., "Bifurcation Buckling of Circular Cylindrical Shells Under Uniform External Pressure," *AIAA Journal*, Vol. 27, No. 2, 1989, pp. 242-248.
- Lou, K. A., and Yaniv, G., "Buckling of Circular Cylindrical Composite Shells Under Axial Compression and Bending Loads," *Journal of Composite Materials*, Vol. 25, No. 2, 1991, pp. 162-187.
- Thangaratnam, R. K., Palaninathan, R., and Ramachandran, J., "Thermal Buckling of Laminated Composite Shells," *AIAA Journal*, Vol. 28, No. 5, 1990, pp. 859, 860.
- Huang, S. C., and Hsu, B.S., "Vibration of Spinning Ring-Stiffened Thin Cylindrical Shells," *AIAA Journal*, Vol. 30, No. 9, 1992, pp. 2291-2298.
- Narita, Y., Ohta, Y., Yamada, G., and Kobayashi, Y., "Analytic Method for Vibration of Angle-Ply Cylindrical Shells Having Arbitrary Edges," *AIAA Journal*, Vol. 30, No. 3, 1992, pp. 790-796.
- Heyliger, P. R., and Jilani, A., "Free Vibration of Laminated Anisotropic Cylindrical Shells," *Journal of Engineering Mechanics*, Vol. 119, No. 5, 1993, pp. 1062-1077.
- Birman, V., "Axisymmetric Bending of Generally Laminated Cylindrical Shells," *ASME Journal of Applied Mechanics*, Vol. 60, No. 1, 1993, pp. 157-162.
- Miyazaki, N., and Hagihara, S., "Bifurcation Buckling of Circular Cylindrical Shells Subjected to Axial Compression During Creep Deformation," *ASME Journal of Pressure Vessel Technology*, Vol. 115, No. 3, 1993, pp. 268-274.
- Chaudhuri, R. A., and Abu-Arja, K. R., "Closed-Form Solutions for Arbitrary Laminated Anisotropic Cylindrical Shells (Tubes) Including Shear Deformation," *AIAA Journal*, Vol. 27, No. 11, 1989, pp. 1597-1605.

¹⁴Christoforou, A. P., and Swanson, S. R., "Analysis of Simply-Supported Orthotropic Cylindrical Shells Subject to Lateral Impact Loads," *ASME Journal of Applied Mechanics*, Vol. 57, No. 2, 1990, pp. 376–382.

¹⁵Butkovskiy, A. G., *Structure Theory of Distributed Systems*, Wiley, New York, 1983.

¹⁶Yang, B., "Distributed Transfer Function Analysis of Complex Distributed Parameter Systems," *ASME Journal of Applied Mechanics*, Vol. 61, No. 1, 1994, pp. 84–92.

¹⁷Yang, B., and Tan, C. A., "Transfer Functions of One-Dimensional

Distributed Parameter Systems," *ASME Journal of Applied Mechanics*, Vol. 59, No. 4, 1992, pp. 1009–1014.

¹⁸Zhou, J., and Yang, B., "Analysis of Ring-Stiffened Cylindrical Shells," *ASME Journal of Applied Mechanics* (to be published).

¹⁹Donnell, L. H., "Stability of Thin-Walled Tubes under Torsion," NACA-TR479, 1933.

²⁰Markus, S., *The Mechanics of Vibrations of Cylindrical Shells*, Elsevier, Amsterdam, 1989.

²¹Yamaki, N., *Elastic Stability of Circular Cylindrical Shells*, North-Holland, Amsterdam, 1984.